A monolithic silicon telescope for hadron beams: numerical and experimental study of the effect of ΔE detector geometry on microdosimetric distributions

Stefano Agosteo[a,b], Giovanni D'Angelo[a,b], Alberto Fazzi[a,b], Maria Vittoria Introini[a,b] and Andrea Pola[a,b*]

[a]Politecnico di Milano, Dipartimento di Energia, Sezione Nucleare, via Ponzio 34/3, 20133 Milano, Italy; [b]Istituto Nazionale di Fisica Nucleare, Sezione di Milano, via Celoria 16, 20133 Milano, Italy

1. Introduction

The microdosimetric approach was recently proposed in literature for improving the quality assessment of hadrontherapy beams [1-3]. For carbon ion beams, in particular, this approach could improve the description of the local energy deposition within tissues, allowing a better exploitation of the properties of hadron beams. Tissue equivalent proportional counters (TEPCs) are the main instruments employed to estimate the beam quality for the full tissue-equivalence (both the walls and the filling gas of the detector are tissue-equivalent), the accurate response to primary and secondary charged particles over a wide energy range and the isotropic angular response. Nevertheless, the routine use of TEPCs in clinical practice is obstructed by the complexity of the associated systems.

Recently, Agosteo et al. proposed and tested the possibility of performing hadron beam characterizations by exploiting a detection system based on a silicon device, the Monolithic Silicon Telescope, alternative to to the TEPC from a practical point of view, being simple, easy-of-use, transportable, cheap and versatile [4].

The Monolithic Silicon Telescope consists of a surface ΔE detector 2 μm in thickness coupled to an E detector about 500 μm in thickness made out of a single silicon wafer [5]. The telescopic structure of ΔE-E devices, in particular the presence of the E stage below the ΔE stage, offers the opportunity of measuring event by event the residual energy of particles with range lower than about 500 μm. A feasibility study carried out with mono-energetic neutrons and clinical protons demonstrated the capability of this silicon device of reproducing microdosimetric spectra similar to those obtained by TEPCs [4,6].

Two different monolithic silicon telescopes which differ in the complexity of the ΔE detector geometry were designed and fabricated in collaboration with ST-Microelectronics. In order to characterize the performance of the two typologies with hadron beams, two sample devices were irradiated with 62 AMeV carbon ions. These tests allowed to study the influence of the geometrical structure of ΔE detector on the spectra acquired by the silicon device.

2. Materials and methods

The study of the effect of ΔE detector geometry on microdosimetric distributions was carried out by irradiating two different sample detectors with 62 AMeV carbon ions at the "Test" facility of the

*Corresponding author. Email: andrea.pola@polimi.it

superconducting cyclotron of the Laboratori Nazionali del Sud - National Institute of Nuclear Physichs (INFN-LNS). A picture of the irradiation set-up is shown in **Figure 1**. The primary beam passes through a 15 μm tantalum foil used for current monitoring and is extracted through a kapton (Ka) window. A collimator, a monitor chamber and a final brass collimator 2.5 cm in diameter are used to shape and monitor the delivered beam. The overall distance between the Ka window and the final collimator is about 140 cm. The depth dose profile of the carbon beam is usually measured with a water phantom through a plane parallel advanced PTW Markus ionization chamber, referred as reference chamber in the following.

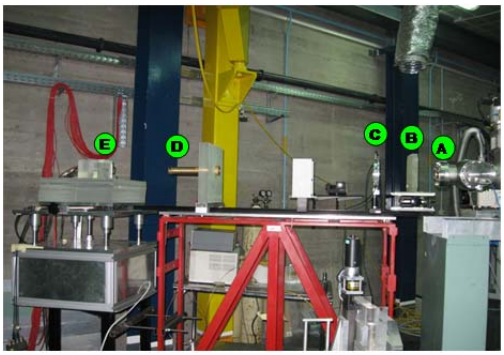

Figure 1. Beam line exploited for the irradiations of the monolithic silicon telescope: A) kapton window, B) collimator, C) monitor chamber, D) final brass collimator E) PMMA phantom in which the detector was placed.

The measurements were performed by inserting two different sample detectors in a polymetilmetacrylate (PMMA) phantom at different depths. The two devices differ in the ΔE detector design: i) a standard prototype (MST in the following) with a ΔE stage constituted by a single pad about 1x1 mm^2 in sensitive area (**Figure 2a**) and ii) a new device (SMST in the following) having a ΔE stage geometrically segmented in a matrix of 7000 micrometric cylinders (about 9 μm in diameter and about 1.9 μm in height) connected in parallel to give an effective area of about 0.5 mm^2 (**Figure 2b**) [6].

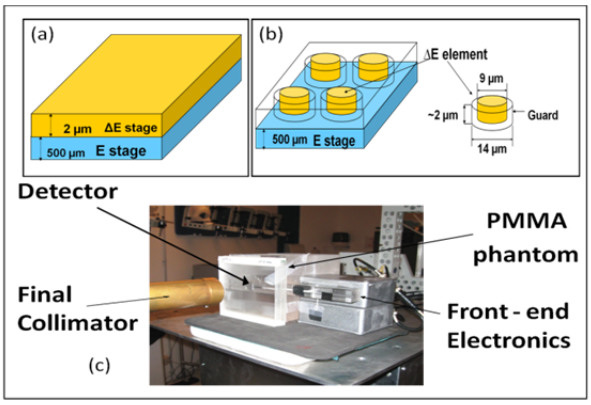

Figure 2. Sketch of the MST (a) and the SMST (b). The devices were irradiated within a PMMA phantom (c) and the different depths were obtained by placing the required layer of PMMA in front of the devices.

The dimensions of the cylinders and of the guard rings correspond to minimum values achievable by the fabrication technology. The ΔE and E stages were fully depleted by applying a bias voltage of 6 V and 150 V, respectively.

3. Experimental results

The MST and the SMST were irradiated across and beyond the Bragg peak, at the positions A-D and E-H of **Figure 3**, respectively. The aim was to study the response of the detector to carbon ions and to their fragments by acquiring and processing the distributions of the energy $E_{\Delta E}$ imparted per event in the ΔE stage versus that deposited in the E stage, E_E. The lineal energy spectra were calculated by correcting the energy imparted spectra measured with the silicon ΔE detector for tissue-equivalence and for shape-equivalence, with the procedures described in details in reference [6].

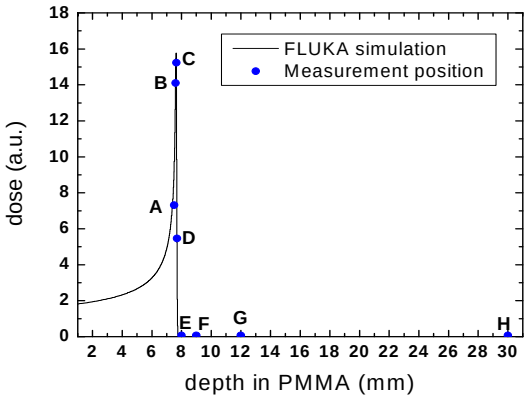

Figure 3. Measurement points adopted for the irradiations of the MST and the SMST: 7.5mm (A), 7.6 mm (B), 7.65 mm (C), 7.7 mm (D), 8 mm (E), 9 mm (F), 12 mm (G), 30 mm (H).

3.1. Measurements across the Bragg peak (points A-D)

Positions A-D in Figure 3 refer to nominal PMMA depths of 7.5, 7.6, 7.65 and 7.7 mm respectively.

The lineal energy spectra obtained with the MST and the SMST devices are directly compared in **Figures 4a-d**. The position of the main peak and the values of the carbon edge agree fairly well. At low y-values the spectra collected by the SMST are characterized by a tail which is populated by about 50% of total events. This contribution may be ascribed to two distinct effects: i) the track length distribution of the cylindrical ΔE elements of the array detector; ii) charge sharing between the ΔE collecting electrodes and their surrounding guards.

3.2. Measurements beyond the primary beam (pointsE-H): contribution of fragments

Measurement positions E-H in Figure 3 correspond to depths in PMMA of about 8, 9, 12 and 30 mm, respectively. 62 AMeV primary carbon ions do not reach these depths and only fragmentation products are

present. The lineal energy distributions obtained with the MST and the SMST devices at measurement points E-H are shown in **Figure 5e-h**. The lineal energy threshold resulted to be about 20 keV μm^{-1}. The distributions are characterized by a complex structure due to the presence of different kind of particles at different energies. The contribution of helium ions and protons are located at low y-values (less than 50 keV μm^{-1}) owing to their high energy, while boron ion events extend up to 700 keV μm^{-1}. This value resulted to be lower than the expected one (i.e. 1000 keV μm^{-1}, from stopping-power tables) owing to the use of an averaged correction factor for tissue equivalence correction.

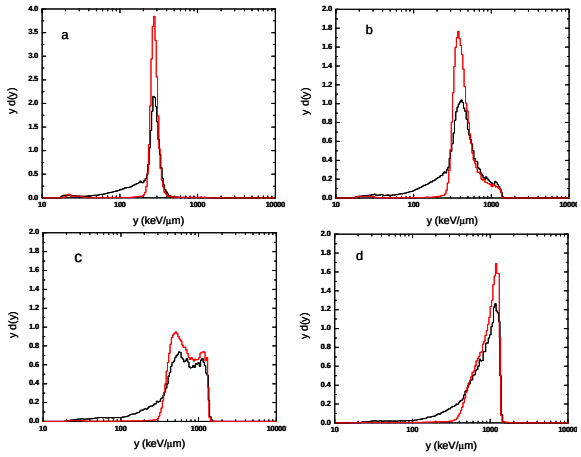

Figure 4. Lineal energy spectra measured with the MST (black line) and SMST (red line) at PMMA depths of 7.5 (a), 7.6 (b), 7.65 (c) and 7.7 mm (d) across the Bragg peak.

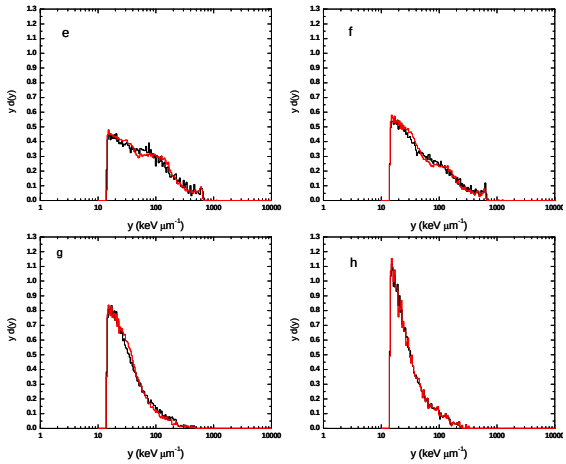

Figure 5. Lineal energy spectra measured with the MST (black line) and SMST (red line) at PMMA depths of 8 (e), 9 (f), 12 (g) and 30 mm (h), beyond the Bragg peak.

4. Numerical study with the FLUKA code

In order to reproduce and deeply analyze the experimental results, in particular to investigate the effects mentioned above, a detailed numerical study based on Monte Carlo simulations was carried out through the FLUKA code version 2012, a recent release able to transport heavy ions at energies lower than 100 AMeV (the older lower transport limit) by exploiting the new Boltzmann Master Equation model.

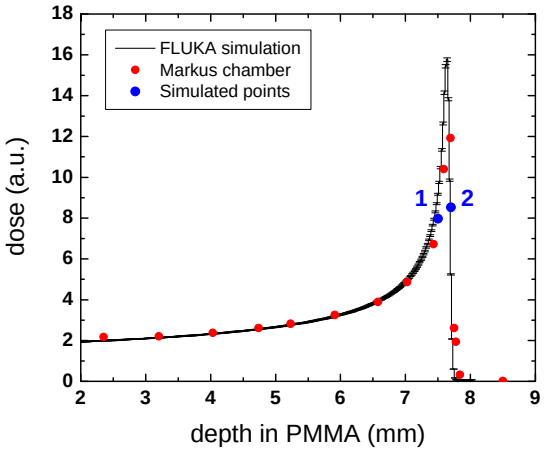

Figure 6. Depth dose profile measured with the reference chamber (red points) together with that obtained with the FLUKA simulations (black curve). Points 1 and 2 (blue points) refer to the PMMA depths selected for the simulations of the MST device.

The geometry of the beam lines used, firstly simulated in details, were simplified with good approximation in order to optimize the computing time. The energy of the primary beam was set to 55.3 AMeV instead of 62 AMeV, to take into account the energy degradation through the beam delivery system and primary carbons were transported in vacuum at the phantom surface. As shown in **Figure 6**, the depth dose profile obtained with the simplified simulation agrees well with the one measured through the reference chamber.

The energy imparted in the two detector stages at different depths in phantom was calculated on an event-by-event basis by multiple scattering transport.

The lineal energy distributions obtained by simulating the MST and the SMST devices at measurement points 1 and 2 selected for the numerical analysis are shown in **Figure 7** together with the corresponding experimental results. In the case of the MST device, results of Monte Carlo simulations agree fairly well with those obtained experimentally. For the SMST, the calculated distributions differ from those measured at low-y values. This disagreement cannot be ascribed to approximations in the simulated geometry or radiation transport, since all parameters were selected to have an accurate calculation. Therefore, the differences between simulated and measured spectra are probably due to events in the experimental distribution which are affected by border effects, in particular by charge sharing between the ΔE electrode and the guard. This effect, negligible when using the MST, becomes important with the SMST, for which the ratio between the area and the perimeter of the ΔE electrode is low.

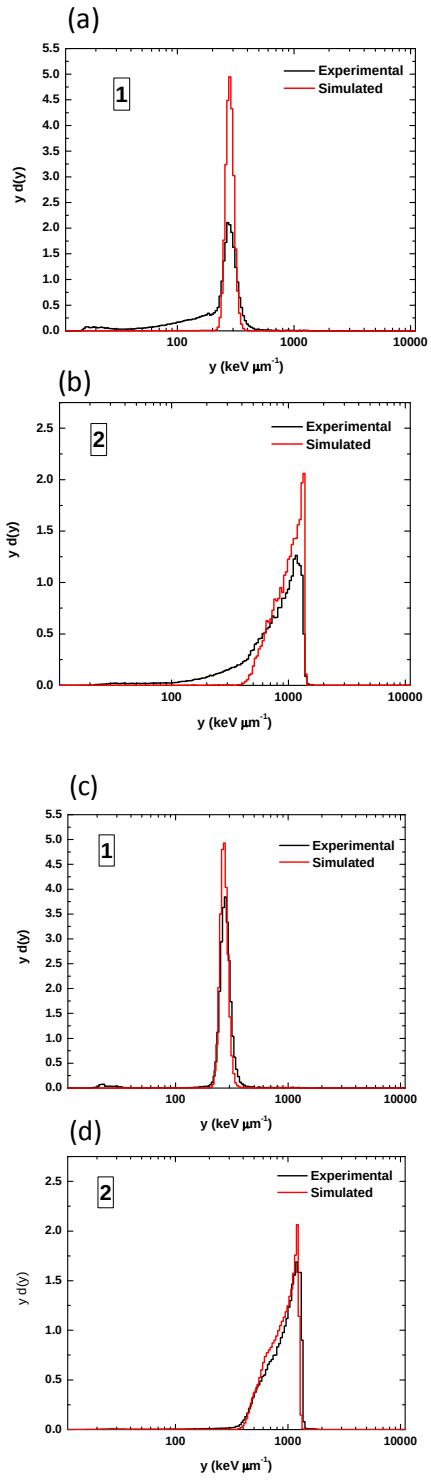

Figure 7. Lineal energy spectra measured (black) and simulated (red) by considering as the detector the SMST (a and b) or the MST (c and d). 1 and 2 are the measurement positions.

Border effects can be clearly observed only in the primary beam (points A-D) because the impinging particles are characterized by a narrow energy distribution peaked at high lineal energy values. Measurements at points E-I do not show differences between MST and SMST since the border effect contribution is spread over the entire spectrum and located mainly at energies below the threshold (see Figure 5).

5. Conclusions

Two monolithic silicon telescopes which differ in the geometrical structure of the ΔE detector were characterized with 62 AMeV carbon ions. Microdosimetric distributions of the hadron beam were measured at different depths within a PMMA phantom.

The analysis of the measured and calculated spectra highlighted a tail on the microdosimetric distributions measured by the segmented monolithic silicon telescope at low lineal energies. Those effects can be associated to charge sharing between the ΔE collecting electrodes and their surrounding guards. Further investigations are needed to better investigate the charge sharing effect on the microdosimetric distributions obtained by the SMST and to identify strategies to minimize its influence. This will be carry out through ion beam analysis technique.

References

[1] H. G. Menzel, P. Pihet and A. Wambersie, Microdosimetric specification of radiation quality in neutron radiation therapy, *Int. J. Radiat. Biol.* 57 (1990), pp.865-883.

[2] G. Coutrakon, J. Cortese, A. Ghebremedhin, J. H. Hubbard, J. Johanning, P. Koss, G. Maudsley, C. R. Slater and C. Zuccarelli, Microdosimetry spectra of the Loma Linda proton beam and relative biological effectiveness comparison, *Med. Phys*. 24 (1997).

[3] L. De Nardo, D. Moro, P. Colautti, V. Conte, G. Tornielli and G. Cuttone, Microdosimetric investigation at the therapeutic proton beam facility of CATANA, *Radiat. Prot. Dosim.* 110 (2004), pp.681-686.

[4] S. Agosteo, G. D'Angelo, A. Fazzi, M. V. Introini, A. Pola, G.A.P. Cirrone and G. Cuttone, Study of a silicon telescope for solid state microdosimetry: preliminary measurements at the therapeutic proton beam line of CATANA, *Radiat. Meas.* 45 (2010), pp.1284-1289.

[5] S. Tudisco, F. Amorini, M. Cabibbo, G. Cardella, G. De Geronimo, A. Di Pietro and G. Fallica, A new large area monolithic silicon telescope, *Nucl. Instrum. Meth.* A 426 (1999), pp.436-445.

[6] S. Agosteo, P.G. Fallica, A. Fzii, M.V Introini, A. Pola and G. Valvo, A pixelated Silicon Telescope for Solid State Microdosimetry. *Radiat. Meas.* 43 (2008), pp.585-589.